Hindawi
Journal of Nanomaterials
Volume 2018, Article ID 7526869, 10 pages
https://doi.org/10.1155/2018/7526869

Research Article

The Systems of Volume-Localized Electron Quantum Levels of Charged Fullerenes

Rafael V. Arutyunyan and Alexander V. Osadchy

Nuclear Safety Institute of the Russian Academy of Sciences (IBRAE RAN), 52 Bolshaya Tulskaya Street, Moscow 115191, Russia

Correspondence should be addressed to Alexander V. Osadchy; aosadchy@kapella.gpi.ru

Received 5 June 2018; Accepted 1 October 2018; Published 3 December 2018

Academic Editor: Jean M. Greneche

The existence of a system of short-lived, discrete, volume-localized electron quantum levels in positively charged fullerenes is theoretically and numerically demonstrated using the example of fullerenes C_{60} and C_{20}. Unlike experimentally and theoretically well-studied electron states localized in a thin surface layer, these electron states are due to the flat part of the Coulomb potential of a positively charged fullerene sphere. The energy width of the system of such discrete volume-localized levels depends on the charge and increases with increasing charge. For $C_{60}{}^{+1}$, the energy width is 0.16 a.u. and increases up to 0.9 a.u. for fullerene $C_{60}{}^{+10}$. Thus, the electrons captured on these discrete levels of fullerene form a sort of short-lived superheavy "nanoatom" or "nanoion," in which the electrons are localized inside a positively charged spherical "nucleus" with an atomic mass of 240 a.u. for C_{20} and 720 a.u. for C_{60}. Numerous published papers have demonstrated theoretically and experimentally the existence of metastable positively charged C_{60} fullerenes with a charge of +10 or more, which suggests the possibility of experimental observation of the considering system of volume-localized electronic states. In conclusion, questions are discussed and estimates are made of the possibility of generating coherent radiation at these transitions.

1. Introduction

Fullerenes are a well experimentally and theoretically investigated object. A large number of papers have been devoted to the study of the electronic states of neutral fullerenes [1–7]. Various methods have been used to study the stability and the mechanism of the decay of charged fullerenes. A number of experimental studies demonstrate the existence of a metastable $C_{60}{}^{+n}$ cation with charges up to +10 and more [8–14]. Most of these results were observed in the collision of fullerenes with highly charged ions. Also, it was shown in the works that charged C_{60} molecules are most likely to decay by emission of C^{+2} [9–11] and with a lower probability of C^{+4} [10, 11]. The largest value of the C_{60} charge, observed experimentally, is +12 [12]. This result was achieved by irradiating C_{60} molecules with intense laser radiation.

A theoretical study of the stability limit of fullerene molecules is presented in papers using different approaches [9–11, 13]. In the work based on the Dirac-Fock-Slater simulation [13], the limiting charge is +13. The application of the molecular dynamics method, together with a simplified approach based on the density functional theory, demonstrates the limiting charge from +16 to +19 [14]. Calculations of the lifetime of highly charged (+10 or more) fullerenes are in the range of microseconds [15] to seconds [16].

In this paper, the existence of a system of short-lived, discrete, volume-localized electron quantum levels in positively charged fullerenes is shown theoretically and numerically in the example of fullerenes C_{60} and C_{20} on the basis of the theoretical approach presented in [17].

2. Methods and Approaches

The modeling was carried out using two main approaches. As the first, a numerical solution of the Schrodinger equation for a spherically symmetric potential in the nodal approximation was applied. Most calculations were carried out using the calculation zone 50 a.u. and the number of nodes is 1000.

The second approach was based on the density functional theory (DFT) [18], which was implemented in the software

package Quantum Espresso [19]. The electron wave functions are decomposed in a plane wave basis. To reduce the dimension of the plane wave basis, the pseudopotential method was used. In the study of nanosized materials, the supercell method with a translation vector length of 100 a.u. was used to exclude the interaction between fullerenes. As the pseudopotential, the Perdew-Wang norm-conserving potentials [20] were used in the framework of the local density approximation (LDA). The basis takes into account plane waves with energies less than 40 Ry. The structure was optimized using a method based on the Broyden-Fletcher-Goldfarb-Shanno algorithm. The positions of the ions varied to a state where the interatomic forces became less than 10^{-4} Ry/a.u., and the parameters of the unit cell varied to values at which the stress in the cell became less than 0.5 Kbar. Calculations were carried out on a high-performance cluster computer K-100 of the MV Keldysh Mathematics Institute of Russian Academy of Sciences.

3. Results and Discussion

The simplest physical model for describing the potential of a charged fullerene is the widely used approximation of the charged sphere field potential:

$$U(r) = -ZU_{\Phi}(r),$$
$$U_{\Phi}(r) = \begin{cases} \dfrac{1}{R_f}, & \text{when } r \le R_f, \\ \dfrac{1}{r}, & \text{when } r \ge R_f, \end{cases} \quad (1)$$

where Z is the positive charge and R_f is the fullerene radius.

For convenience, we used a dimensionless system of units, assuming the electron mass $m = 1$, the electron charge $e = 1$ and $\hbar = 1$. In general, our attention will be directed to the study of the fullerene C_{60}, whose radius we take $R_f = 6.627$ a.u. [1].

A simple estimate of the discrete energy levels of an electron in such a potential can be obtained from the known solutions of the Schrödinger equation for a spherical rectangular well of depth $U_0 = Z/R_f$. Within this sphere ($0 \le r \le Rf$), the solution of the Schrödinger equation is described by a spherical Bessel function $\chi = j_l(\xi r/R_f)$ that satisfies the boundary conditions at zero $\chi(0) = 0$. Then, outside the well ($R_f < r < \infty$), the solution that satisfies $\chi(\infty) = 0$ is represented by the spherical Henkel function $\chi = h_l(i\eta r/R_f)$. The parameters ξ and η are algebraically related:

$$\xi^2 + \eta^2 = 2U_0R_f^2, \quad (2)$$

and determine the discrete energy levels:

$$E_n = -\frac{\eta^2}{2R_f^2} = -U_0 + \frac{\xi^2}{2R_f^2}. \quad (3)$$

Table 1: Energy levels of a rectangular spherically symmetric well for $Z = 1$.

l	Analytical	Numeric	
	Energy, a.u.	Very deep well Energy, a.u.	Finity depth Energy, a.u.
0	−0.039	−0.03951	−0.08491
1			−0.02238

Table 2: Energy levels of a rectangular spherically symmetric well for $Z = 5$.

l	Analytical	Numeric	
	Energy, a.u. (analytical)	Very deep well Energy, a.u. (numeric)	Finity depth Energy, a.u.
0	−0.642	−0.64259	−0.66606
1	−0.525	−0.52419	−0.57418
2	−0.376	−0.37602	−0.45974
0	−0.305	−0.30886	−0.40861
3	−0.199	−0.19842	−0.32414
1	−0.075	−0.07506	−0.23738
4			−0.23738
2			−0.05561
0			−0.02611

The values of the parameters ξ and η are fixed by the condition of continuity of the wave function for $r = Rf$. For $l = 0$, it is means

$$\eta = -\xi \mathrm{ctg}\xi. \quad (4)$$

Tables 1 and 2 show the electron levels of the spherical potential well at $Z = 1$ and $Z = 5$, obtained from (3). Also in the tables, for comparison, the results of numerical solutions of the Schrödinger equation for a very deep well $U_0 \gg (1/2R_f^2)$ and a well of finite depth are shown.

To calculate the energy spectrum of electrons in the potential well (1), we solved the standard Schrödinger equation for the radial component of the wave function:

$$\frac{d^2\chi}{dr^2} - \frac{l(l+1)}{r^2}\chi + 2(E - U(r))\chi = 0, \quad \chi(r) = rR(r). \quad (5)$$

The calculations have been performed in the nodal approximation with the number of nodes $n = 1000$.

Comparing the results shown in Tables 1 and 2, it can be seen that the discrete energy levels obtained by an analytical solution of the Schrödinger equation for an infinitely deep spherically symmetric well and by numerical solution in the nodal approximation coincide with good accuracy. Numerical solutions for a well of finite and infinite depth coincide for the lowest-lying energy levels and expectedly begin to diverge with increasing energy.

A characteristic feature of the system of discrete levels corresponding to the smooth part of the potential (2) is that the electron wave functions corresponding to them are localized in the fullerene volume, in contrast to the well-

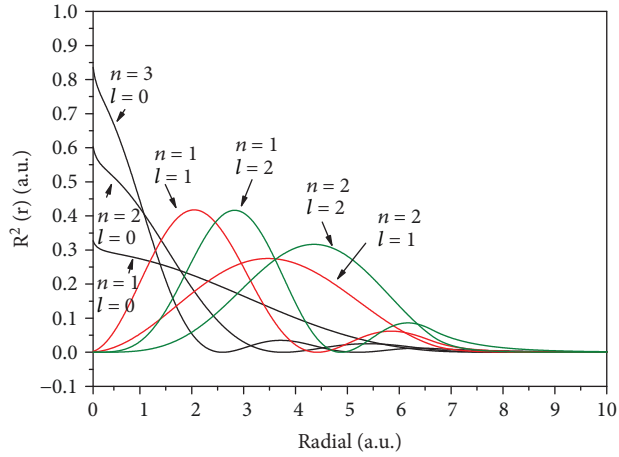

Figure 1: Wave function radial component squares for electron states of a rectangular spherically symmetric well of finite depth at $Z = 5$ received as a result of the numerical calculations of the Schrödinger equation (5).

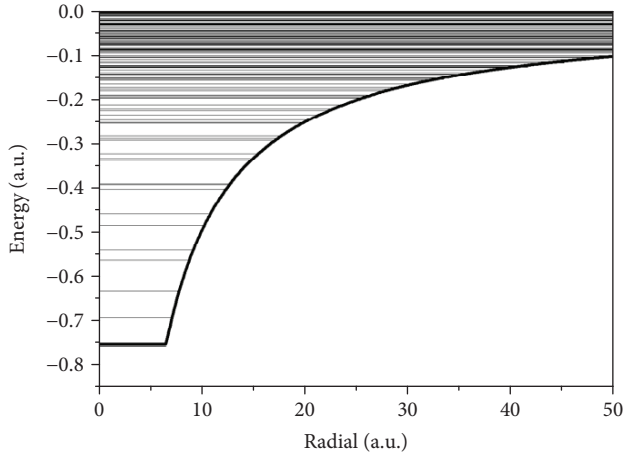

Figure 2: Energy levels of a spherically symmetric potential (1) at $Z = 5$ received as a result of the numerical calculations of the Schrödinger equation (5).

studied surface-localized electronic states (Figure 1). The number of such states increases with increasing depth of the potential, which occurs with the growth of the fullerene charge Z (Tables 1 and 2).

To solve the stationary Schrödinger equation (5) for an electron in the potential well (1), we can use a numerical solution for a spherically symmetric potential in the nodal approximation. Figure 2 shows the numerical calculation results obtained for the charge $Z = 5$ for the number of nodes $n = 1000$ and the calculation region $r \leq 50$ a.u.

3.1. Potential of the Charged Fullerene Taking into Account the Coulomb Field and the Analytic Approximation of the Well on the Surface in the Model of the Jelly. For the subsequent consideration of the discrete electronic levels of a charged fullerene, we take into account the potential as the sum of the Lorentz potential of the surface layer in the jelly

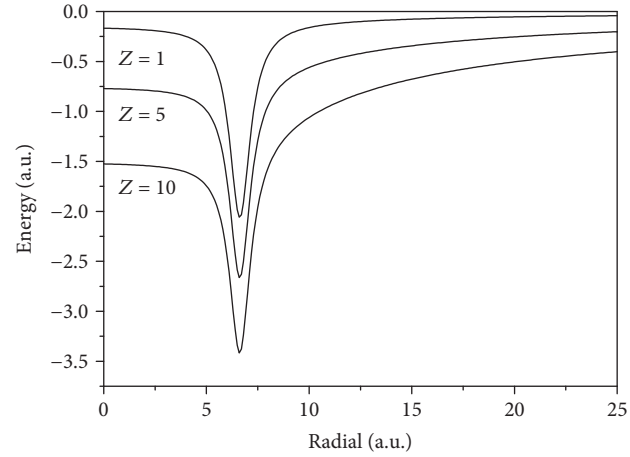

Figure 3: Analytical potential of fullerene (5) for various Z.

model [21] and the Coulomb potential of the positively charged sphere.

$$U(r) = -\frac{V}{(r-R)^2 + d^2} - ZU_{\Phi}(r), \tag{6}$$

where in accordance with [17], $V = 0.711$, $R = 6.627$, $d = 0.610$, and Z is the positive charge of fullerene.

In this case, we neglect the influence of the Coulomb potential (1) on the potential (5).

The potentials (5) for different Z are shown in Figure 3. The potential in the center of the fullerene becomes deeper as the charge increases. For $Z = 1$, $U(0) = -0.17$ a.u., whereas in the case of $Z = 5$, $U(0) = -0.77$ a.u. and $U(0) = -1.52$ a.u. at $Z = 10$. As a result, we obtain two types of electronic states: localized on a thin sphere of fullerene and with a volumetric localization of the electron.

This is clearly seen in the results of numerical solutions of the Schrödinger equation for an electron in the potential (5) for different Z. Figure 4 shows the spectra of a charged fullerene at $Z = 1$ and $Z = 5$. Tables 3 and 4 contain a set of discrete electron states for a charged fullerene at $Z = 1$ and $Z = 5$, respectively. For comparison, Tables 3 and 4 show discrete electronic states for the Coulomb potential of the charged sphere (1) for $Z = 1$ and $Z = 5$, respectively.

It can be seen from the tables that the numerical values of the energy of the discrete excited levels of the Coulomb potential (1) and the values of the levels of the total potential (5) located above the plane part of the Coulomb potential are fairly close.

Figure 5 shows the results of numerical calculations of the squares of the radial components of the wave functions of a spherically symmetric potential (5) at $Z = 5$. As can be seen from the graphs, along with well-known surface-localized levels in the energy spectrum of electrons, there are volume-localized excited levels.

3.2. The Calculation of Energy Levels of Discrete States of a Charged C_{60} Fullerene on the Basis of the Electron Density Functional. To compare the results obtained, numerical

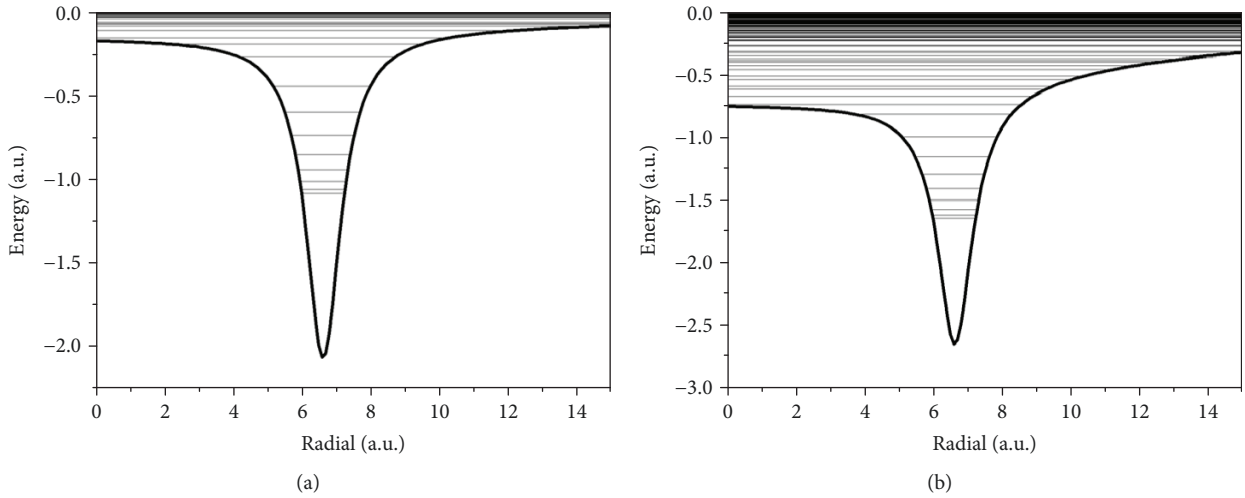

Figure 4: Energy levels of a spherically symmetric potential (5) at $Z = 1$ (a) and $Z = 5$ (b) received as a result of the numerical calculations of the Schrödinger equation (5).

Table 3: Energy levels of a spherically symmetric potential (1) and potential (5) for $Z = 1$ received as a result of the numerical calculations of the Schrödinger equation (5).

Potential (1)			Potential (5)		
n	l	Energy, a.u.	n	l	Energy, a.u.
			1	0	−1.05864
			1	1	−1.01158
			1	2	−0.94142
			1	3	−0.84862
			1	4	−0.73372
			1	5	−0.59734
			1	6	−0.44019
			1	7	−0.26313
			1	8	−0.18781
			2	0	−0.14966
1	0	−0.11313	2	2	−0.10578
1	1	−0.08074	2	0	−0.07869
2	0	−0.05527	3	9	−0.06724
1	2	−0.05132	1	3	−0.06289
2	1	−0.04079	2	1	−0.05440
3	0	−0.03175	3	0	−0.03975
1	3	−0.03104	4	2	−0.03907
2	2	−0.02903	3	1	−0.02987
3	1	−0.02427	4	4	−0.02805
1	4	−0.01974	2	3	−0.02762

Table 4: Energy levels of a spherically symmetric potential (1) and potential (5) for $Z = 5$ received as a result of the numerical calculations of the Schrödinger equation (5).

Potential (1)			Potential (5)		
n	l	Energy, a.u.	n	l	Energy, a.u.
			1	0	−1.66521
			1	1	−1.64135
			1	2	−1.59381
			1	3	−1.52295
			1	4	−1.42919
			1	5	−1.31308
			1	6	−1.17518
			1	7	−1.01614
			1	8	−0.83671
			2	0	−0.75648
1	0	−0.69530	2	1	−0.69254
1	1	−0.63561	1	9	−0.63773
1	2	−0.56490	2	2	−0.61415
2	0	−0.54226	3	0	−0.55998
1	3	−0.48600	2	3	−0.53094
2	1	−0.45972	3	1	−0.48054
1	4	−0.40322	2	4	−0.44853
3	0	−0.39317	1	10	−0.42032
2	2	−0.39088	3	2	−0.40964
3	1	−0.33771	4	0	−0.39563

calculations of the potentials of charged fullerenes were carried out using a method based on the electron density functional theory. Numerical three-dimensional potentials for the electron in a charged fullerene are obtained using Quantum Espresso code [19]. In contrast to potential (5), these dependencies take into account the positions of each carbon atom, which leads to a violation of the spherical symmetry. It is necessary to distinguish two characteristic cross sections of the potentials obtained: passing through the center of the fullerene and through the carbon atom and passing through the middle of the segment connecting neighboring atoms. Figure 6 contains the analytical potentials for the C_{60} fullerene at $Z = 3$ and $Z = 5$, as well as the cross sections calculated numerically by the DFT potential, passing through the carbon atom and through the center of a segment between neighboring atoms.

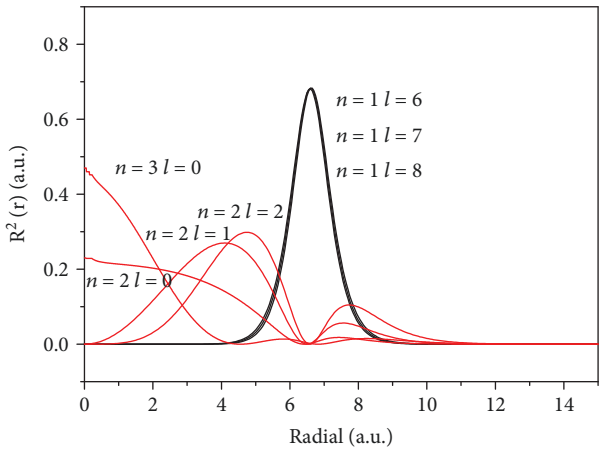

FIGURE 5: Squares of the wave function radial component of the spherically symmetric potential (5) states at $Z = 5$ received as a result of the numerical calculations of the Schrödinger equation (5).

It can be seen that the maximum depth of the potential well obtained using DFT, similar to potential (5), decreases with increasing Z. The value of the potential in the center of the fullerene is higher than the analytical approximation (5) that we have used. The potential well located on the radius of the fullerene is less deep and wider. The reason for this difference is the relatively rough approximation within the jelly model, whereas the DFT makes it possible to more accurately calculate the potential, taking into account all fullerene atoms.

We consider the solution of the Schrödinger equation in a spherical symmetric field, where potentials calculated using the DFT method were used as the field potential. The cross sections for the potentials under consideration were taken through the carbon atoms and passing through the center of a segment between the neighboring atoms. Despite the fact that the real field of fullerenes is not centrally symmetric, this approach may be justified because we are most interested in states with energies above the potential well in the center of the charged fullerene. These states are the least subject to the lack of symmetry.

Figure 7 shows the examples of the obtained electronic states for C_{60} fullerene with charges +1, +5, and +10.

Figure 8 presents the results of numerical calculations of the squares of the radial components of the wave functions of a spherically symmetric potential calculated for a C60 fullerene with a charge of +5. Analogous to the case of the analytical potential (5), it can be seen from the graphs that along with the well-known surface-localized levels in the energy spectrum of the electrons, there are volume-localized excited levels.

As can be seen from Figures 7 and 8, the energy spectra of the electrons and wave functions calculated using the potential obtained by the method based on the electron density theory are close to the results obtained in solving the Schrödinger equation for analytical potentials (5). The principal difference between the results obtained for the potential (5) and the calculated one using DFT is observed for states located below the potential in the center of the fullerene.

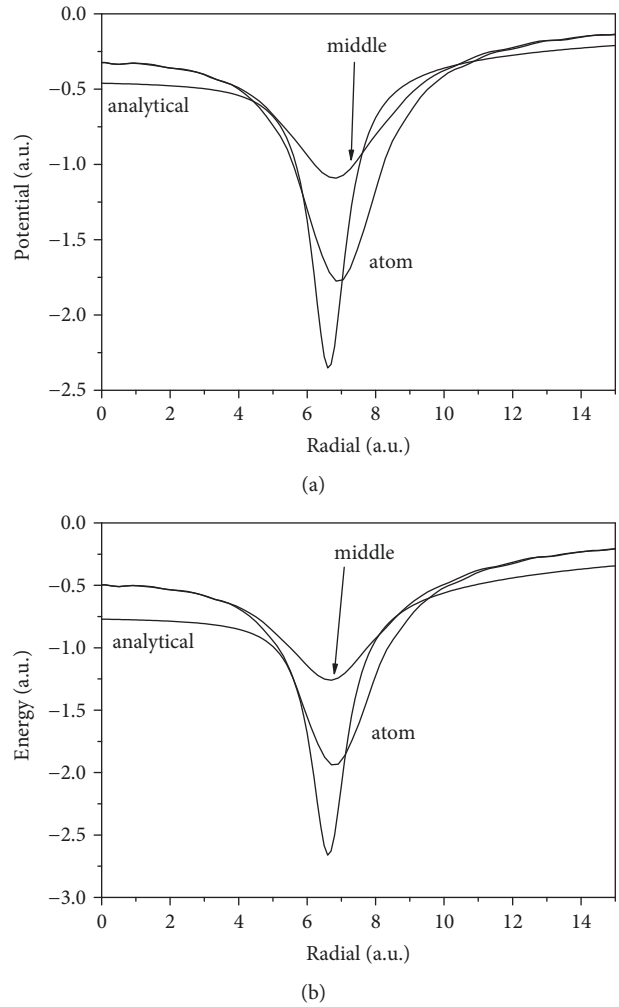

FIGURE 6: Comparison of the analytical potential of the charged fullerene (5) at $Z = 3$ (a) and $Z = 5$ (b) with cross sections of the calculated potential at $Z = 3$ and $Z = 5$, passing through the atom of carbon (*atom*) and through the center of the segment connecting the neighboring atoms (*middle*).

These states are localized within the thin sphere of the fullerene surface. Due to the fact that DFT takes into account the positions of all fullerene atoms in an explicit form, the potential is not spherically symmetric, as in the case with potential (5). At the same time, states with energies greater than the potential at the center of the fullerene are localized in the fullerene volume, and the calculated potential for the DFT is practically spherically symmetric, analogous to (5). This is clearly seen in Figure 8, which represents the calculated squares of the wave functions obtained as a result of the solution of the Schrödinger equation for states located at the level of the boundaries of occupied and free states at the bottom of the potential well at the center of the fullerene and above the bottom of the potential well. Data for fullerene C_{60} with charge +10 are presented. Fullerene with other charges demonstrates similar results.

Since the potential equations used by us do not take into account the anisotropy of the distribution of the charged fullerene field, to confirm the obtained data, we calculated the

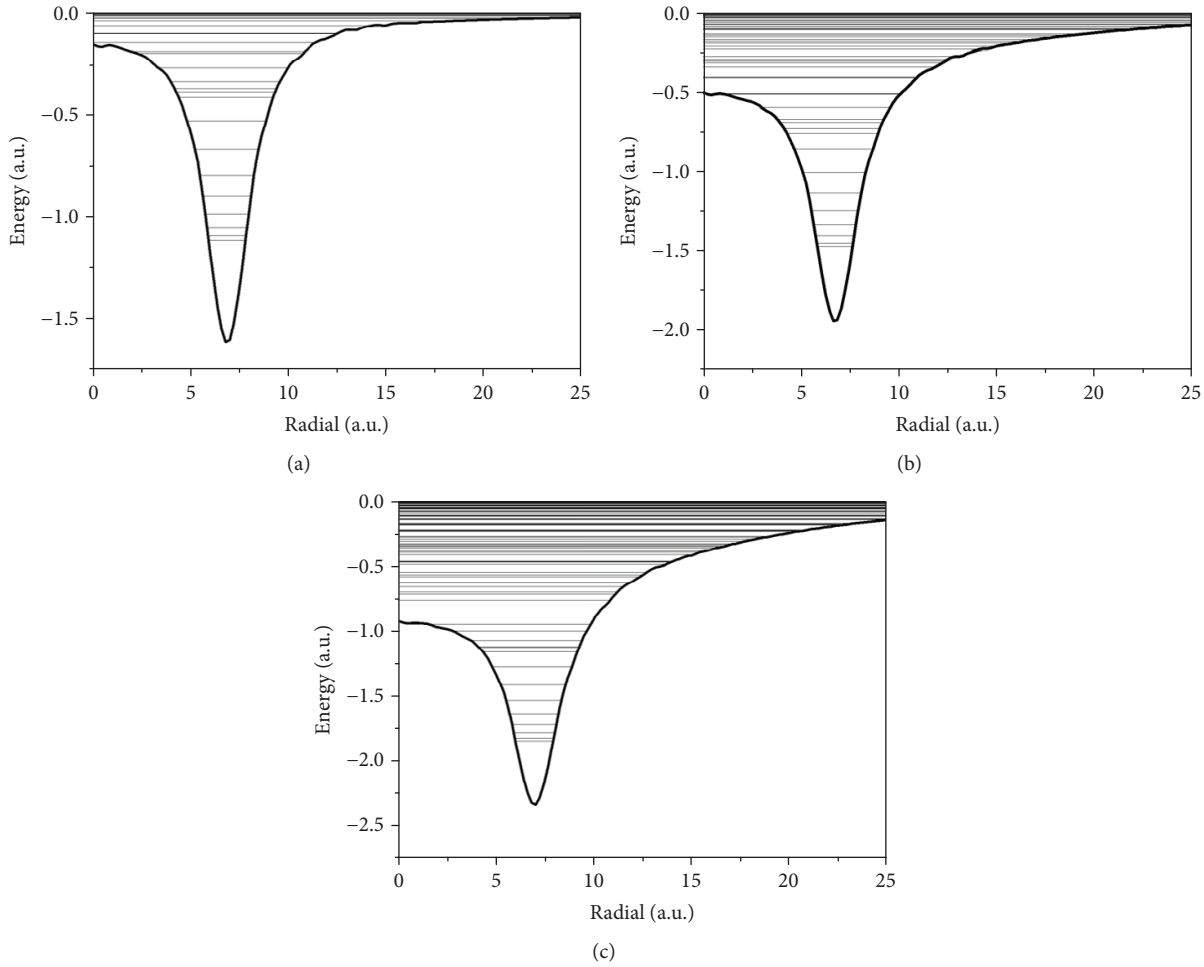

Figure 7: Energy levels in spherical symmetric potential received as a result of the numerical calculations of the Schrödinger equation (5) for the C_{60} fullerene with charge +1 (a), +5 (b), and +10 (c). The spherically symmetric potential is obtained in the form of a cross section of a three-dimensional potential calculated with the use of DFT. The cross section was taken through a carbon atom.

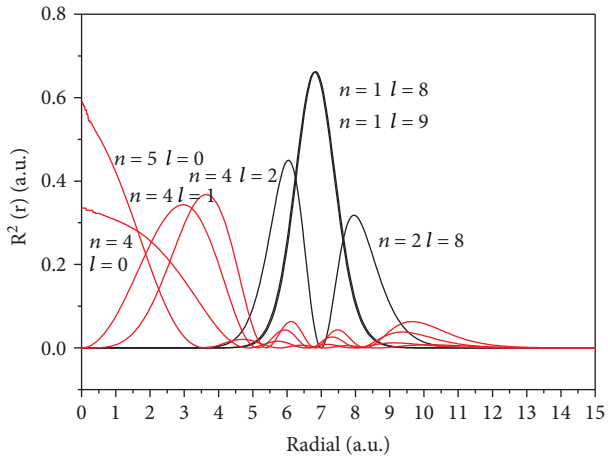

Figure 8: Squares of the radial component of the wave functions of states of a spherically symmetric potential received as a result of the numerical calculations of the Schrödinger equation (5) for C_{60} fullerene at $Z = 5$. The spherically symmetric potential is obtained in the form of a cross section of a three-dimensional potential calculated with the use of DFT. The cross section was taken through a carbon atom.

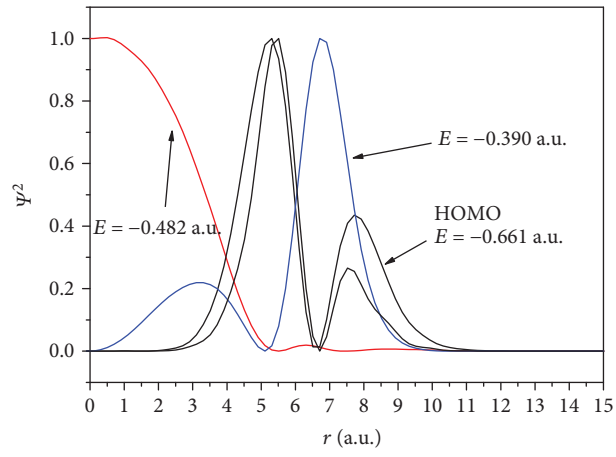

Figure 9: Wave function squares obtained with the usage of the DFT computations for a charged C_{60} fullerene with $Z = 5$.

3D dependences of the squares of the wave functions of one-electron C60 fullerene states with a charge of +5. Calculations were carried out using the theory of the electron density functional taking into account the position of all fullerene

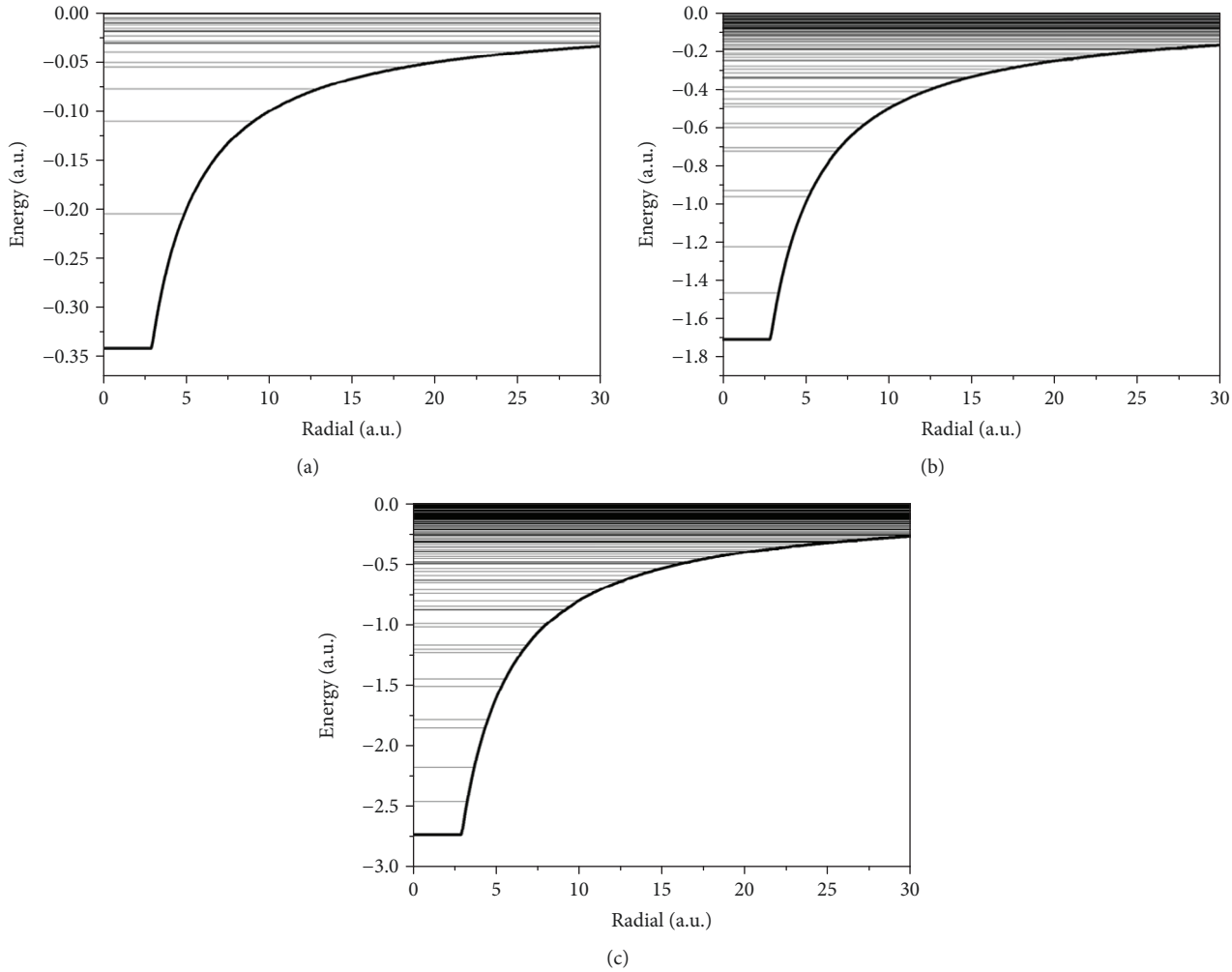

Figure 10: Energy levels of a spherically symmetric potential (1) received as a result of the numerical calculations of the Schrödinger equation (5) for C_{20} fullerene at $Z = 1$ (a), $Z = 5$ (b), and $Z = 8$ (c).

Table 5: Energy levels of a spherically symmetric potential (1) at $Z = 1$, 5, and 8 received as a result of the numerical calculations of the Schrödinger equation (5).

$Z = 1$			$Z = 5$			$Z = 8$		
n	l	Energy, a.u.	n	l	Energy, a.u.	n	l	Energy, a.u.
1	0	−0.2042	1	0	−1.4612	1	0	−2.4539
1	1	−0.1104	1	1	−1.2205	1	1	−2.1725
2	0	−0.0776	1	2	−0.9592	1	2	−1.8511
1	2	−0.0552	2	0	−0.9271	2	0	−1.7761
2	1	−0.0506	2	1	−0.7247	1	3	−1.5060
3	0	−0.0401	1	3	−0.7038	2	1	−1.4462
1	3	−0.0311	3	0	−0.6009	3	0	−1.2280
2	2	−0.0310	2	2	−0.5781	2	2	−1.1997
3	1	−0.0290	1	4	−0.4919	1	4	−1.1673
4	0	−0.0238	3	1	−0.4780	3	1	−1.0172

atoms realized in the Quantum Espresso software package. The cross sections of the 3D dependences obtained are shown in Figure 9. The 3D potential calculation taking into account the potential anisotropy and the simplified spherically symmetric potential (Figure 8) demonstrate similar results, which justifies the simplified approximation we use.

3.3. Discrete Energy Levels of Charged C_{20} Fullerene. Similar results can be obtained for other types of fullerenes, including those for C_{20}. According to [22], the radius of a given fullerene can be taken equal to $R = 2.93$ a.u. The electron states obtained by numerically solving the Schrödinger equation for a spherically symmetric potential (1), applied to C_{20}, are shown in Figure 10, the values of 10 states with the lowest energy are shown in Table 5.

Calculation by a method based on the theory of the electron density functional theory makes it possible to obtain potentials similar to the case of a charged C_{60} fullerene. The electron states in the spherical symmetric potential calculated by the DFT method for C_{20} fullerene with charge $Z = 5$ and $Z = 8$ are shown in Figure 8. It is worth noting that the radius of C_{20} increases with increasing of charge. Thus, according to [22], the radius of neutral fullerene is 2.93 a.u.; at the same time, according to calculations using DFT, shown in Figure 11, with charge $Z = 5$, it increases to 3.8 a.u. and

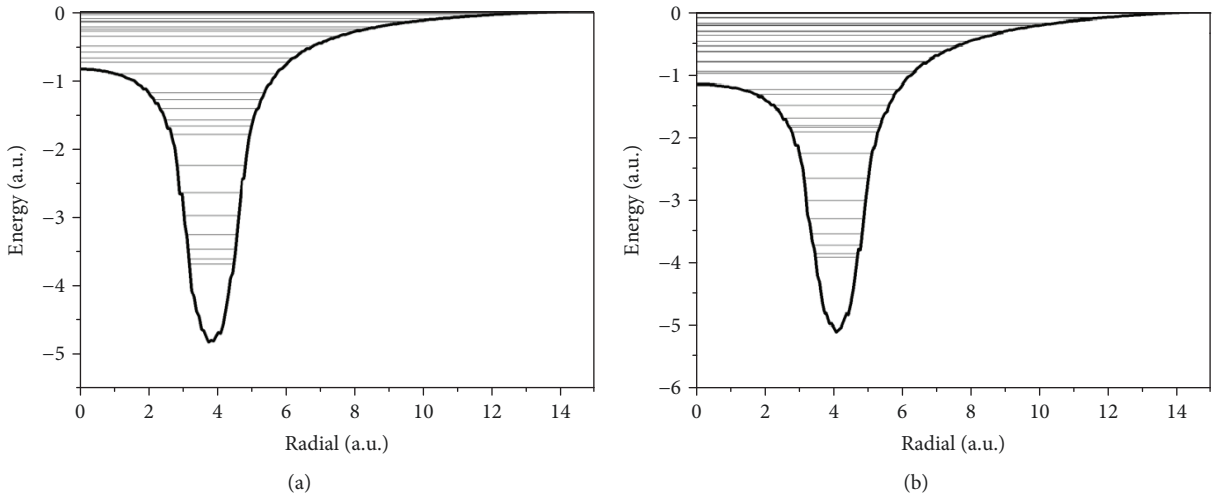

FIGURE 11: Energy levels in spherically symmetric potential received as a result of the numerical calculations of the Schrödinger equation (5) for C20 fullerene with a charge of +5 (a) and +8 (b). The spherically symmetric potential is obtained in the form of a cross section of a three-dimensional potential calculated with the use of DFT. The cross section was taken through a carbon atom.

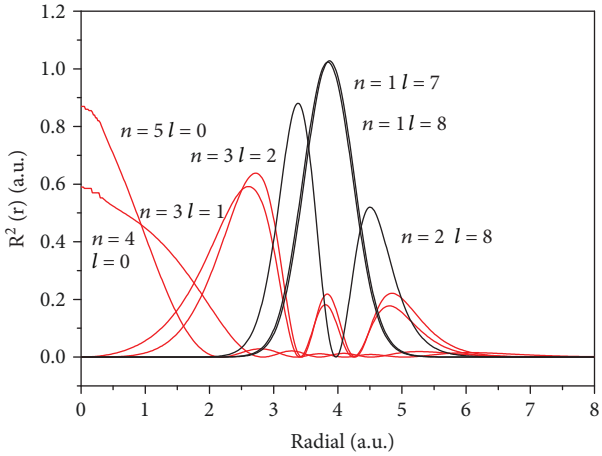

FIGURE 12: Squares of the radial component of the wave functions of the states of a spherically symmetric potential received as a result of the numerical calculations of the Schrödinger equation (5) for C20 fullerene at $Z = 5$. The spherically symmetric potential is obtained in the form of a cross section of a three-dimensional potential calculated with the use of DFT. The cross section was taken through a carbon atom.

at $Z = 8$ up to 4.14 a.u. Figure 12 presents the results of numerical calculations of the squares of the radial components of the wave functions of a spherically symmetric potential calculated for a C_{20} fullerene with a charge of +5. At the same time, we do not consider the question of the stability and lifetime of such positively charged fullerenes.

Thus, similar to C_{60} fullerene, the calculations are given for the analytical potential (1) applied to C_{20}, as well as numerical solutions of the Schrödinger equation for spherically symmetric potentials of charged C_{20} fullerenes obtained by the DFT method, along with well-studied electron states localized within the thin sphere fullerene; there are states localized in the volume.

4. Conclusion

In this paper, we demonstrated on the basis of theoretical and numerical calculations, using the example of fullerenes C_{60} and C_{20}, the existence of a system of short-lived discrete volume-localized quantum levels of electrons in positively charged fullerenes. Thus, the electrons captured on these discrete levels of fullerene form a sort of short-lived "nanoatom" or "nanoion," in which the electrons are localized inside a positively charged spherical "nucleus."

The results obtained provide a consistent qualitative picture for charged fullerenes. To clarify our very approximate results, of course, further research is needed on the basis of microscopic calculations, as well as experimental measurements.

To estimate the lifetime of such levels, one can use the well-known formula for the photon emission rate:

$$P_{ij} = \frac{\omega^3}{3\pi\varepsilon_0\hbar c^3}\left|d_{ij}\right|^2, \tag{7}$$

where ω is the emission frequency and d_{ij} is the matrix element of dipole transition from the initial (j) to the final (i) state.

One can estimate the magnitude of d_{ij} for transitions between volume-localized levels of charged fullerenes as eR. A simple numerical estimate, taking $R = 6.627$ a.u. for fullerene C_{60}, leads to

$$P_{ij} = \frac{4(6.627)^2}{3\alpha}\frac{c}{\lambda}\left(\frac{\Delta E}{m_e c^2}\right)^3. \tag{8}$$

Thus, it is possible to obtain for various ΔE: $P_{ij}(\Delta E = 1\,\text{eV}) = 4.67 \cdot 10^7\,\text{s}^{-1}$ and $P_{ij}(\Delta E = 10\,\text{eV}) = 4.67 \cdot 10^{10}\,\text{s}^{-1}$. This gives an estimate of the lifetime of states in the range from 21 ns to 21 ps, which is much smaller than the estimated lifetimes

of charged fullerenes and suggests the possibility of experimental confirmation of the existence of volume-localized discrete levels.

Experimental confirmation of the existence of these volume-localized discrete levels would be of great interest for experimental research and practical tasks, including the development of new sources of coherent radiation in a wide range of wavelengths.

To estimate the inverse population value n_{ij}, which is necessary to reach the threshold for the generation of coherent radiation at volume-localized levels of fullerenes, we use the following simple expression:

$$\mu_\omega L_{\text{abs}} \gg 1, \tag{9}$$

where

$$\mu_\omega = \frac{\lambda^2}{2\pi} n_{ij} \frac{\Delta\omega}{\Delta\omega_{\text{sp}}}, \tag{10}$$

where μ_ω is the resonance amplification factor per unit length; L_{abs} is the photon loss length; $\Delta\omega$ is full broadening of the emission line due to the Doppler effect, collisional broadening and broadening due to nonradiative losses; $\Delta\omega_{\text{sp}}$ is the width of dipole spontaneous emission line; λ is the transition wavelength between i and j levels; and ω is the emission frequency at the transition $i - j$.

$$n_{ij} \gg \frac{2\pi}{\lambda^2 L_{\text{abs}}} \frac{\Delta\omega_{\text{sp}}}{\Delta\omega}, \qquad \Delta\omega \approx \Delta\omega_{\text{dop}} + \Delta\omega_{\text{col}} + \Delta\omega_{\text{nrad}}. \tag{11}$$

The value $L_{\text{abs}} \sim (1/n\sigma_{\text{abs}})$, where n is the volume density of fullerenes. According to experimentally measured values in fullerene pairs of C_{60} [23], $\sigma_{\text{abs}} \sim 10^{-15}\text{cm}^2$ in the wavelength range of 200–400 nm.

To reach the generation threshold of coherent radiation in the optical range, the estimate of the volume density of the inverted population n_{ij} at the fullerene density $n = 10^{14} - 10^{15}$ cm^{-3} gives the value of $10^{12} - 10^{13}$ cm^{-3}.

Data Availability

The data used to support the findings of this study are available from the corresponding author upon request.

Conflicts of Interest

The authors declare that there is no conflict of interest regarding the publication of this paper.

References

[1] M. S. Dresselhaus, G. Dresselhaus, and P. C. Eklund, "Fullerenes," *Journal of Materials Research*, vol. 8, no. 8, pp. 2054–2097, 1993.

[2] B. Mignolet and F. Remacle, "Time-efficient computation of the electronic structure of the C_{60} super-atom molecular orbital (SAMO) states in TDDFT," *AIP Conference Proceedings*, vol. 1790, article 020015, 2016.

[3] A. M. Polubotko and V. P. Chelibanov, "Withdrawal of electrodynamical forbiddance and peculiarities of the sers spectra in fullerene C_{70}," *Optics and Spectroscopy*, vol. 124, no. 4, pp. 483–488, 2018.

[4] B. V. Lobanov and A. I. Murzashev, "Optical absorption of fullerene C_{60} within the concept of a strongly correlated state," *Russian Physics Journal*, vol. 59, no. 6, pp. 856–861, 2016.

[5] S. Saito and A. Oshiyama, "Cohesive mechanism and energy bands of solid C_{60}," *Physical Review Letters*, vol. 66, no. 20, pp. 2637–2640, 1991.

[6] F. Negri, G. Orlandi, and F. Zerbetto, "Low-lying electronic excited states of Buckminsterfullerene anions," *Journal of the American Chemical Society*, vol. 114, no. 8, pp. 2909–2913, 1992.

[7] A. Oshiyama, S. Saito, N. Hamada, and Y. Miyamoto, "Electronic structures of C_{60} fullerides and related materials," *Journal of Physics and Chemistry of Solids*, vol. 53, no. 11, pp. 1457–1471, 1992.

[8] T. Nagaya, T. Nishiokada, S. Hagino et al., "Producing multicharged fullerene ion beam extracted from the second stage of tandem-type ECRIS," *Review of Scientific Instruments*, vol. 87, no. 2, article 02A723, 2016.

[9] H. Cederquist, J. Jensen, H. T. Schmidt et al., "Barriers for asymmetric fission of multiply charged C60 fullerenes," *Physical Review A*, vol. 67, article 062719, 2003.

[10] S. Tomita, H. Lebius, A. Brenac, F. Chandezon, and B. A. Huber, "Energetics in charge-separation processes of highly charged fullerene ions," *Physical Review A*, vol. 67, no. 6, 2003.

[11] G. Senn, T. D. Mark, and P. Scheier, "Charge separation processes of highly charged fullerene ions," *The Journal of Chemical Physics*, vol. 108, no. 3, pp. 990–1000, 1998.

[12] S. Martin, L. Chen, A. Denis, R. Bredy, J. Bernard, and J. Désesquelles, "Excitation and fragmentation of $C_{60}^{r+}(r = 3 - 9)$ in $Xe^{30+} - C_{60}$ collisions," *Physical Review A*, vol. 62, no. 2, article 022707, 2000.

[13] J. Jensen, H. Zettergren, H. T. Schmidt et al., "Ionization of C_{70} and C_{60} molecules by slow highly charged ions: a comparison," *Physical Review A*, vol. 69, no. 5, 2004.

[14] A. Rentenier, A. Bordenave-Montesquieu, P. Moretto-Capelle, and D. Bordenave-Montesquieu, "Asymmetric fission and evaporation of C_{60}^{r+}(r=2–4) fullerene ions in ion–C_{60} collisions: I. Proton results," *Journal of Physics B: Atomic, Molecular and Optical Physics*, vol. 37, no. 12, pp. 2429–2454, 2004.

[15] H. Zettergren, G. Sánchez, S. Díaz-Tendero, M. Alcamí, and F. Martín, "Theoretical study of the stability of multiply charged C_{70} fullerenes," *Journal of Chemical Physics*, vol. 127, no. 10, article 104308, 2007.

[16] R. Sahnoun, K. Nakai, Y. Sato, H. Kono, Y. Fujimura, and M. Tanaka, "Theoretical investigation of the stability of highly charged C60 molecules produced with intense near-infrared laser pulses," *Journal of Chemical Physics*, vol. 125, no. 18, article 184306, 2006.

[17] R. V. Arutyunyan, *Theoretical Investigation of Electronic Properties of Highly Charged Fullerenes. Systems of Discrete Short-Lived Volume-Localized Levels*, Nuclear Safety Institute RAS IBRAE, Moscow, 2018.

[18] M. C. Payne, M. P. Teter, D. C. Allan, T. A. Arias, and J. D. Joannopoulos, "Iterative minimization techniques for *ab initio* total-energy calculations: molecular dynamics and conjugate

gradients," *Reviews of Modern Physics*, vol. 64, no. 4, pp. 1045–1097, 1992.

[19] P. Giannozzi, S. Baroni, N. Bonini et al., "Quantum ESPRESSO: a modular and open-source software project for quantum simulations of materials," *Journal of Physics: Condensed Matter*, vol. 21, no. 39, article 395502, 2009.

[20] J. P. Perdew and Y. Wang, "Accurate and simple analytic representation of the electron-gas correlation energy," *Physical Review B*, vol. 45, no. 23, pp. 13244–13249, 1992.

[21] A. S. Baltenkov, S. T. Manson, and A. Z. Msezane, "Jellium model potentials for the C_{60} molecule and photoionization of endohedral atoms, $A@C_{60}$," *Journal of Physics B: Atomic, Molecular and Optical Physics*, vol. 48, no. 18, article 185103, 2015.

[22] K. D. Sattler, *Handbook of Nanophysics: Clusters and Fullerenes*, CRC Press, 2017.

[23] Q. Gong, Y. Sun, Z. Huang, X. Zhu, Z. N. Gu, and D. Qiang, "Absorption spectrum of gas-phase C_{60} in the 200-400 nm region," *Journal of Physics B: Atomic, Molecular and Optical Physics*, vol. 27, no. 9, pp. L199–L201, 1994.